MYTRIBOS Malaysian Tribology Society
Jurnal Tribologi
Website : jurnaltribologi.mytribos.org e-issn: 2289-7232

Wear detection by sulfides as solid lubricants and thermoelectric materials

Tomohiro Sato [1*], Masaki Yoshihara [2], Kenichi Saitoh [1], Masanori Takuma [1], Yoshimasa Takahashi [1]

[1] Kansai University, Yamate-cho 3-3-35, Suita, Osaka, JAPAN.
[2] Fuji Electric Co., Ltd., Fujicho 1-27, Yokkaichi, Mie, JAPAN.
*Corresponding author: tom_sato@kansai-u.ac.jp

KEYWORDS

Sulfides
Solid lubricant
Thermoelectric material

ABSTRACT

In the field of tribology, sulfides such as molybdenum disulfide are used as solid lubricants. Sulfides also have semiconductor properties and have been studied as thermoelectric conversion materials. In this study, we focus on sulfides used as solid lubricants and investigate a method of sensing the heat generated during friction using a thermoelectric conversion function and using it for wear detection. Using a material made of tin sulfide mixed with graphite, we were able to sense a voltage in response to the progress of friction. In particular, we found an advantage in detection speed compared to other detection mechanisms such as thermocouples, and we report on the details.

1.0 INTRODUCTION

Sulfides are well known as solid lubricants. MoS_2 is one of the most usable solid lubricants in engineering field. Not only MoS_2, but many sulfides are also usable as solid lubricants. These sulfides make friction decrease (Liu et al.,2021, Yin et al.,2019) or stabilize (österle et al.,2016). Cu system sulfides were also developed dry (Ishikawa et al.,2019) and oil (Sato et al.,2021) lubricant conditions. On the other hand, recently sulfides are focused as electricity generation materials, solid state batteries, solar cell and thermoelectric materials (Liu et al.,2018). These functions are based on semiconductor specific of sulfides. In tribotronic field, MoS_2 was often used (Xue et al., 2016). Thermoelectric effect was already researched as wear detection; however, it was not focused material as sulfides, but also focused as bearing system (Zhu et al.,2019).

In this study these two functions, solid lubricant and thermoelectric, of sulfides are focused to express functions at the same time. Especially, the function was applied for wear detection. In

Received 25 July 2024; received in revised form 6 March 2025; accepted 22 March 2025.
To cite this article: Sato et al., (2025). Wear detection by sulfides as solid lubricants and thermoelectric materials. Jurnal Tribologi 45, pp.104-116.

mechanical bearing section these two functions were achieved by using as a mechanical unit (Omoto et al.,2012). In this study these functions were achieved by plan baring.

Detection of wear by using thermoelectric effect, material development was conducted by using sulfide. In this study sulfide played a thermoelectric role and solid lubricant role. Especially, combination of SnS and carbon were indicated superior thermoelectric properties.

By using powder metallurgy method, these materials were sintered as solid lubricants and thermoelectric materials. For the specimen, electrical conductivity that is one of parameters of the thermoelectric function was evaluated.

Our aim of this study is to achieve the wear detecting by using simple solid lubricants, not using other special sensors. In particular, we found an advantage in detection speed compared to other detection mechanisms such as thermocouples, and we report on the details.

2.0 EXPERIMENTAL PROCEDURE

2.1 Combinations of Sn-S and C

In this study, Sn-S system (90 wt%) and C(graphite, 10 wt%) was used. It was named "(Sn-S $)_{0.9}$-$C_{0.1}$". Sn-S contained 66.5 wt% SnS and 23.5 wt% Sn_2S_3 and particle size is between 25 to 150μm. The particle size of graphite is 40μm. Details of selection process of the material on options other than this material were described in section2.2. Here, details of combination on Sn-S and C were described.

The theory of thermoelectric material was evaluated as follows. The theoretical efficiency η of thermoelectric conversion power generation is expressed using the temperature T_H [K]at the high temperature part and the temperature T_L [K]at the low temperature part as follows (Equation (1)).

$$\eta = \frac{T_H - T_L}{T_H} \frac{\sqrt{1 + ZT} - 1}{\sqrt{1 + ZT} + \frac{T_L}{T_H}} \tag{1}$$

The ZT [-] used here is called figure of merit and is determined by the physical properties of the material. ZT is expressed by the Equation (2),

$$ZT = \frac{S^2 \sigma}{\kappa} T \tag{2}$$

where S [V/K] is Seebeck coefficient, σ [S/m] is electrical conductivity, κ [W/mK]is thermal conductivity, and T [K]is the average temperature of the material (T = (T_H+T_L)/2).

In this study, Seebeck coefficient, S=$\Delta V/\Delta T$, was measured as follows. For pin specimen, φ8mm×5mmt, bottom of the specimen was heated by hot plate. Potential difference ΔV[V] between top and bottom of the specimen was measured by the tester. Then ΔT[T] was kept at 80K measured by thermocouple. Electrical conductivity σ [S/m] was calculated, by measuring R[Ω] by the tester for the specimen. Thermal conductivity κ [W/mK] was measured by heat flow sensor using same set up of measuring Seebeck coefficient.

$S^2\sigma$ in the right-hand denominator is called the power factor and indicates the magnitude of emf per unit temperature difference. Since there is a positive correlation between η and ZT, ZT is evaluated as a simple parameter that indicates the efficiency of thermoelectric conversion. The standard values for practical use are considered to be *ZT* = 1.5 to 2 for the utilization of waste heat from automobiles, and *ZT* = 0.5 to 1 for micro power generation. For *ZT* improvement, the combination of $(Sn\text{-}S)_{0.9}\text{-}C_{0.1}$ was better. Because σ will be improved by changing graphite ratio and size based on below theory.

2.2 Selection of Materials and Synthesis Methods

2.2.1 Selection of Materials to Be Used Selection of Materials

Figure 1 shows the maximum *ZT* values obtained for each sulfide semiconductor. Here SnS was made by ampoule tube synthesis (Ishikawa et al., 2019) or mechanochemical methods. Although Cu_5FeS_4 which is one of the superior solid lubricants (Ishikawa et al., 2019) is the material with the largest *ZT* value, $(Sn\text{-}S)_x\text{-}C_y$ is selected as the semiconductor element to be used in the surface state detection sensor envisioned in this study. The reasons are as follows.

The *ZT* value is inferior to that of Cu_5FeS_4 in the present composition and grain size, but the *ZT* value is expected to be improved by adjusting the composition based on the percolation theory.

In SnS, a significant improvement in *ZT* value (about 100 times) has been reported by doping a small amount of Ag, etc. (Bhattacharya et al., 2019). In contrast, no such improvement has been reported for Cu_5FeS_4(Moghaddam et al., 2019), and there is a high possibility that the *ZT* value will be higher than that of Cu_5FeS_4.

This material has already been commercialized as a solid lubricant for brake pads and is trusted to provide a stable coefficient of friction. It is useful as a semiconductor for sensors. The *ZT* value can be adjusted from the two aspects of material particle size and material composition ratio, and it is easy to optimize the *ZT* value and improve the element strength while maintaining the optimum friction characteristics.

The selection of this material is tentative. It is undeniable that the *ZT* value is much lower than those of currently known thermoelectric materials. The discovery of materials with properties superior to those of this material is required.

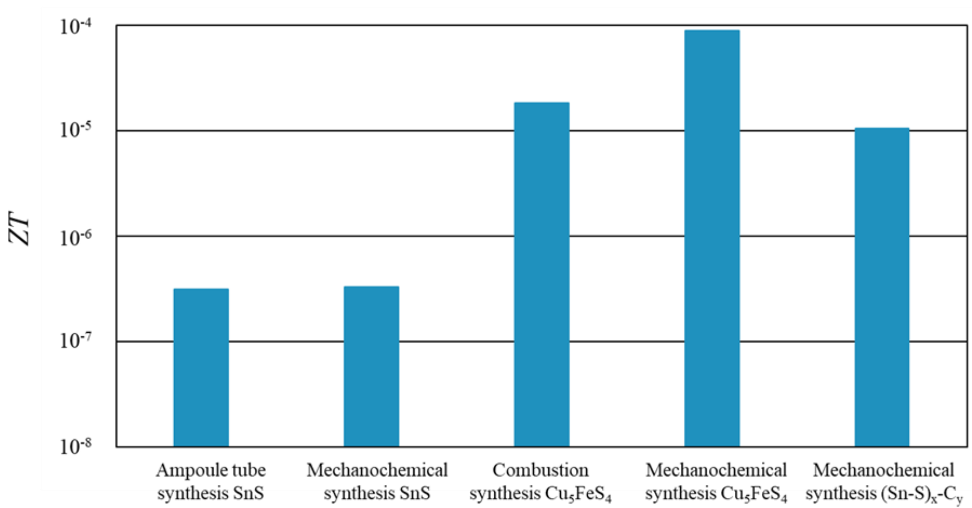

Figure 1: *ZT* of each sulfide.

2.2.2 Composition and Grain Size Optimization of $(Sn\text{-}S)_x\text{-}C_y$ (Carbon-Containing Tin Sulfide)

Since the superiority of $(Sn\text{-}S)_x\text{-}C_y$ has been recognized in the previous sections, we will optimize $(Sn\text{-}S)_x\text{-}C_y$ by considering percolation theory in order to improve the physical properties.

2.2.2.1 Effect of Grain Size on Friction Coefficient

In the previous section, it was found that the physical properties of $(Sn\text{-}S)_x\text{-}C_y$ mainly depend on the percolation theory, and that the *ZT* value can be manipulated from two aspects: material composition ratio and material grain size. In other words, the following two aspects of the *ZT* value can be manipulated.

・Optimization of *ZT* value；Adjustment by material grain size (reduction of C grain size)

・Optimization of frictional properties; Adjustment by material composition ratio

By separating the manipulation methods of *ZT* value and friction property, it is possible to adjust both independently, which facilitates the optimization. However, since this policy assumes that the frictional properties are independent of the material grain size, it is necessary to investigate the effect of the material grain size on the frictional properties.

In order to confirm the above, two types of $(Sn\text{-}S)_{0.9}\text{-}C_{0.1}$ with C grain sizes of 40 μm and 11 μm were prepared, and the coefficients of friction were measured using a journal-type friction tester same type of previous work (Ishikawa et al.,2019). The synthesis methods of the two materials are unified by the supplier. From the results of the measured friction coefficients of the two materials., the friction coefficients are slightly larger for the sample with larger grain size of C, with μ = 0.124 for the 40 μm sample and about μ = 0.098 for the 11 μm sample. This may be attributed to the fact that C in the 40 μm sample is more localized than in the 10 μm sample, and the probability of C on the truth contact surface is lower.

Regarding the effect of particle size on the dispersion of low-friction particles in sintered compacts, it is known from previous studies that samples with lower particle sizes exhibit lower coefficients of friction (Ishikawa et al.,2019).

From the above results, a dependence of the friction coefficient on C grain size was observed for $(Sn\text{-}S)_{0.9}\text{-}C_{0.1}$. However, this result does not affect the independent adjustment of *ZT* values and frictional properties. The friction properties of $(Sn\text{-}S)_x\text{-}C_y$ are optimized by the donor at y = 0.1, and the composition $(Sn\text{-}S)_{0.9}\text{-}C_{0.1}$ contains slightly lower C than the critical volume fraction. In other words, y = 0.1 is preferred for the composition of $(Sn\text{-}S)_x\text{-}C_y$, and the reduction of C grain size is necessary to optimize the electrical conductivity of $(Sn\text{-}S)_{0.9}\text{-}C_{0.1}$. Since this leads to improved frictional properties, this tendency is not a problem.

In a composite material as Sn-S and C in this study consisting of an insulator and a conductor, the factor that controls the conductivity is "the amount of formation of conductive networks (clusters) of conductive particles"(McLachlan.,1985). The amount of cluster formation can be expressed as a function of the "volume fraction of conducting particles" in terms of the cumulative establishment distribution, i.e., the electrical conductivity is expressed as a function of the "volume fraction of conducting particles. This theory is called the percolation theory (McLachlan,1985).

Here, the critical volume fraction φ_c is obtained from the particle size of Sn-S system and C used in this study. The particle size of C is about 25 to 45 μm (Guangxi et al., 2013), and the particle size of Sn-S system is 25 to 150μm. Since it is, the $R_{matrix} / R_{particle}$ shown as bellow is about 4 (The Chemical Society of Japan(ed), 2004).

$$\varphi_c = \frac{(1+n)}{\left(1+n+\left(\frac{\Phi}{2X_c}\right)\left(\frac{\mathrm{R_{matric}}}{\mathrm{R_{particle}}}\right)\right)} \tag{3}$$

Using the experimentally obtained parameters n = 1, Φ = 1.27, X_c = 0.42, in above Eq(3). When the critical volume fraction φ_c is calculated, it is about φ_c = 25%, and when expressed as a mass fraction, it is about 12% (Sato et al.,2022).

2.2 Testing Conditions

Raw mixed powders of $(Sn\text{-}S)_{0.9}\text{-}C_{0.1}$ were pressed at 1.25MPa by hand Newton press as cylindrical pin shape. The size of pin φ8mm×5mmt. Then pressed material was vacuum sintered in 873K.

Mating material was prepared, four types of roughness carbon steel (S45C, JIS) discs with different surface roughness shown in Table 1 by polishing sandpapers. It was evaluated how effect the difference of surface roughness.

The "pin-on-disk tester" is used for rotating discs to conduct thermoelectric power generation tests using frictional heat. For the test, specimens were prepared.

A schematic diagram of the test is shown in Figure 2 and the test conditions are shown in Table 2. Copper wires were extended from the bottom of the specimen and near the sliding part (2 mm below the sliding part) and connected to a data logger to measure the acquired voltage during the test. A thermocouple is placed near the sliding part to measure the temperature at the same time. Coefficient of friction was also evaluated by using strain and torque of the tester. By using the method, this makes it possible to qualitatively evaluate wear.

Table 1: Disk conditions.

Disc	Number of abrasive paper used	Surface roughness (Ra), μm
Disc Ⅰ	80	3.2 - 6.4
Disc Ⅱ	220	1.6 – 3.2
Disc Ⅲ	600	0.8 – 1.6
Disc Ⅳ	1200	0.4

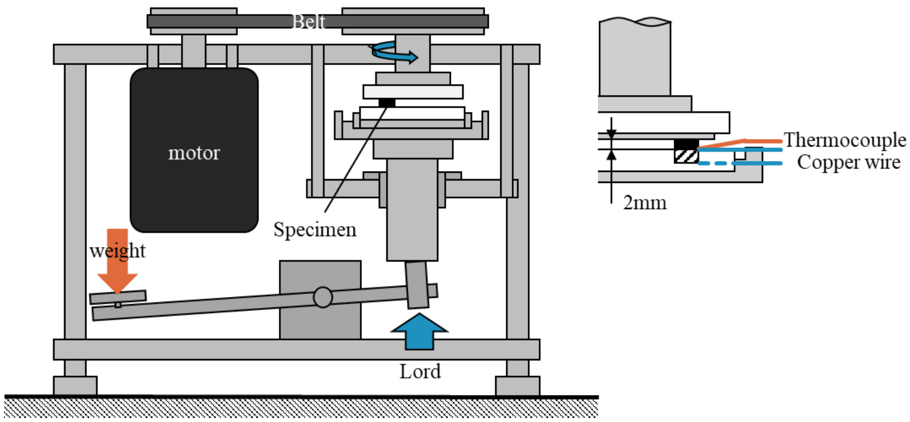

Figure 2: Friction power generation test

Table 2: Friction test conditions.

Environment	**Dry**
Test temperature	RT
Load	2.45 N (0.25 kgf)
Test time	3600 s
Rotation speed	100 rpm
Material of the shaft	S45C (No heat treatment) 340 HV

3.0 RESULTS AND DISCUSSION

3.1 Friction Power Generation Test

Figure 3 shows the relationship between the amount of electricity generated per unit time and the elapsed time for each disk. For all conditions, the amount of power generation increased at a steep gradient from the contact between the disc and $(Sn\text{-}S)_{0.9}\text{-}C_{0.1}$ to a few 10 seconds, and then increased at a low gradient. These results indicate as bellows.

The amount of electricity generated at the point of change in gradient, 10 seconds after the start of the test. The convergence value of the power generation, the power generation after 1800 seconds.

Figure 4 shows the amount of power generated by each disc. No correlation with the surface roughness of the disc was observed in the amount of electricity generated after 10 seconds from the start of the test. This may be due to the fact that the thermoelectric conversion elements used in this test are lubricated with solid lubricant, which has a unique lubrication mechanism compared to oil lubrication and the like. It is known that in the case of solid film lubrication, as the load increases, film formation is promoted and the friction coefficient decreases, and the frictional heat also tends to decrease. In other words, it is possible that the early film formation on the disk with high surface roughness, where the contact area is small and the local load increases, may result in the reduction of the generation of frictional heat. Figure 5 shows the results of optical microscopic observation of the disc surface after 10 seconds from the start of the test. The orange lines indicate that more lubrication film was observed on the discs with rough surfaces, which confirms this possibility.

In the power generation after 1800 seconds from the start of the test, the power generation tended to increase with the surface roughness of the disc. This is considered to be a result of a positive correlation between the surface roughness and the amount of frictional heat generated, since the effect of the aforementioned film growth rate can be ignored after a sufficient growth time of the solid lubricant film. Figure 6 shows the observed results of the disk surface after 1800 seconds. Unlike the result after 10 seconds, the same level of lubrication film formation was observed on both discs.

Here, we consider the usefulness of this sensor as a surface condition sensor for wear detection. Considering that the surface roughness of a disc expresses the degree of defects that occur in real components such as shafts and bearings, the above test results indicate that the disc can be used as a "time monitoring type sensor" that produces a steep slope of power generation immediately after the occurrence of a defect, which suggests the occurrence of a defect, followed by a power generation indicating the degree of the defect after a certain time elapse.

However, the occurrence of electromotive force in such wear conditions as rapid wear, changes in conduction due to contact between the sulfide-impregnated metal (sliding bearing side) and the shaft (metal) and contact in a lubricating oil environment are unknown and will be the subject of future studies.

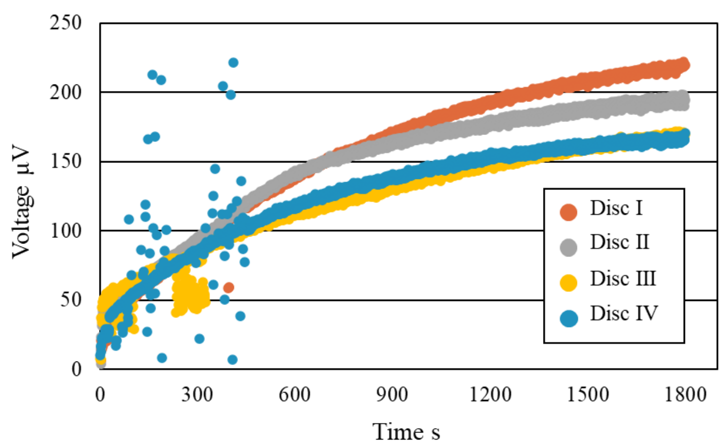

Figure 3: Relationship between elapsed time and power generation in each disc.

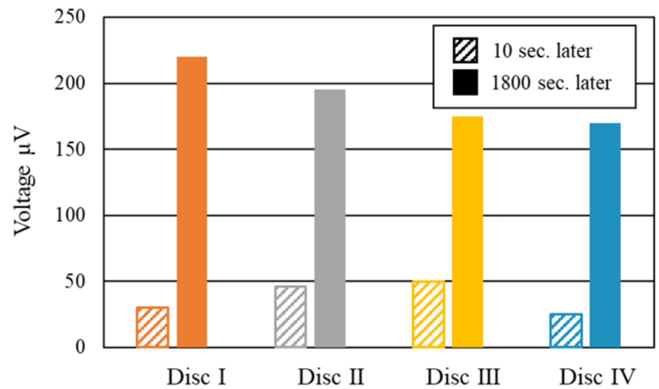

Figure 4: Power generation after 10 seconds and 1800 seconds.

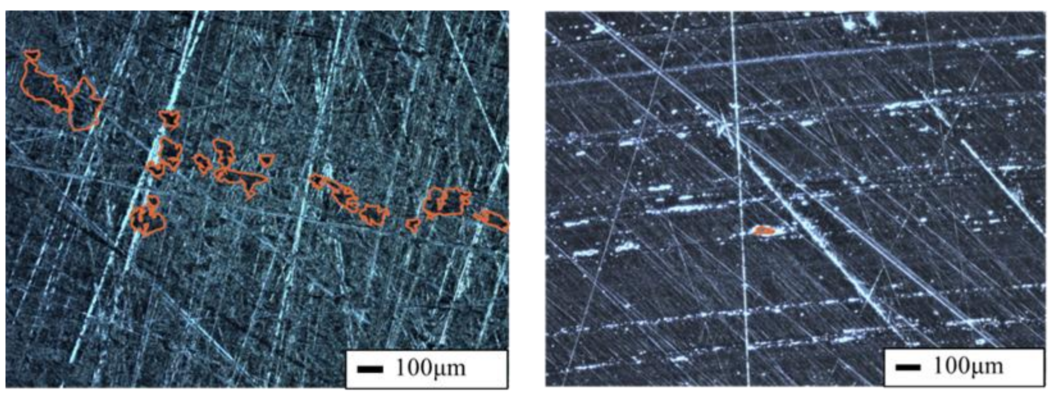

(a) Surface of Disc I (b) Surface of Disc IV

Figure 5: Disc surface after 10 seconds.

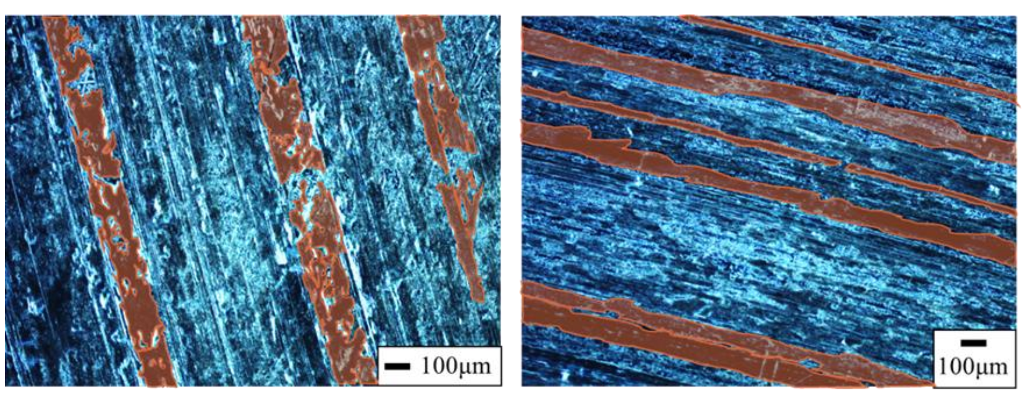

(a) Surface of Disc I (b) Surface of Disc IV

Figure 6: Disc surface after 1800 seconds.

3.2 Results of Temperature Measurement

In order to confirm the superiority of the thermoelectric conversion type sensor, the abnormality detection performance by temperature measurement was evaluated. Figure 7 shows the relationship between temperature and elapsed time for each disk. The evaluation is based on the temperature difference from the beginning to the end of the measurement, as in the frictional heat generation test.

Temperature difference at 10 seconds after the start of the test, which is the point of change of the gradient. Then, temperature difference at 1800 seconds, which is the convergence value of the power generation.

The temperature difference at 1800 seconds, which is the convergence value of the power generation. These values are shown in Figure8.

The temperature difference at 10 seconds after the start of the test could not be evaluated because almost no temperature difference was obtained. This can be attributed to the fact that the thermoelectric conversion type sensor can make direct contact with the object to be detected, while the simple thermocouple cannot make contact with the object, and the speed of temperature information transmission is low. The detection speed was found to be inferior to that of the thermoelectric conversion type sensor.

Temperature difference at 1800 seconds, which is the convergence value of the power generation, showed no correlation with the surface roughness of the disc. Similar to the above, it can be said that this is due to the fact that thermoelectric conversion type sensors can directly contact the object to be detected, whereas simple thermocouples cannot, and the accuracy of the information is also low. The detection accuracy is also found to be inferior to that of the thermoelectric conversion type sensor.

As a result, it is shown that the detection speed and accuracy of the surface state detection in temperature measurement are inferior to those of the thermoelectric conversion type sensors, indicating the superiority of the thermoelectric conversion type sensors.

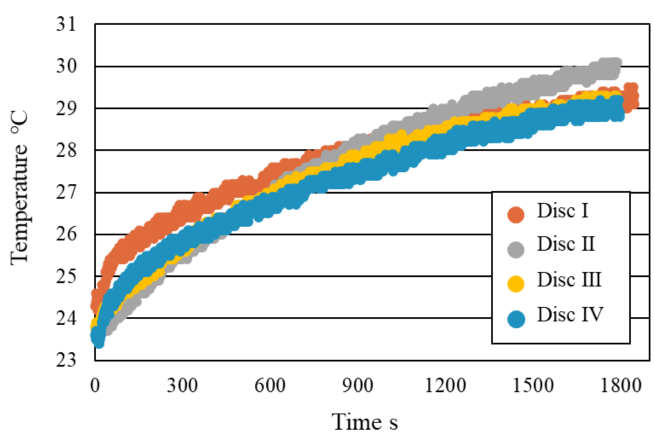

Figure 7: Relationship between elapsed time and measurement temperature in each disc.

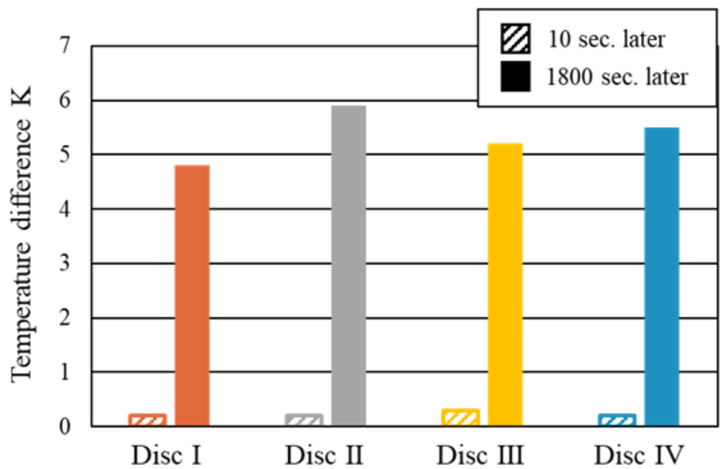

Figure 8: Measurement temperature difference after 10 seconds and 1800 seconds.

3.3 Results of Friction Coefficient Measurement

Continuing from the previous section, it was evaluated that the anomaly detection by measuring the coefficient of friction to confirm the superiority of the thermoelectric sensor. Figure 9 shows the relationship between the coefficient of friction and the elapsed time for each disk. As in the power generation test by frictional heat

Change in the coefficient of friction after 10 seconds from the start of the test, which is the point of change in the gradient and change in the coefficient of friction after 1800 seconds, which is the convergence value of the amount of electricity generated.

Change in the friction coefficient after 1800 seconds, which is the convergence value of the power generation. These values are shown in Figure 10.

For the friction coefficient at 10 seconds after the start of the test, it was possible to estimate the degree of defects to some extent. However, the detection speed is slightly inferior to that of the thermoelectric conversion type sensor, especially for Discs III and IV.

Temperature difference at 1800 seconds, which is the convergence value of the power generation, showed a higher friction coefficient the larger the surface roughness of the disc. The detection accuracy was found to be equivalent to that of the thermoelectric conversion type sensor.

As a result, it was found that the surface condition detection by the friction coefficient measurement is slightly inferior to that by the thermoelectric conversion type sensor in terms of the detection speed and is more accurate than that by the thermoelectric conversion type sensor in terms of the detection accuracy, especially in the initial stage of defect generation. It is presumed that the two types of sensors are used differently because of their different characteristics. In addition, the thermoelectric conversion type sensor has the possibility of independent power supply operation, and thus it can play a dominant role in environments where the power supply is severe.

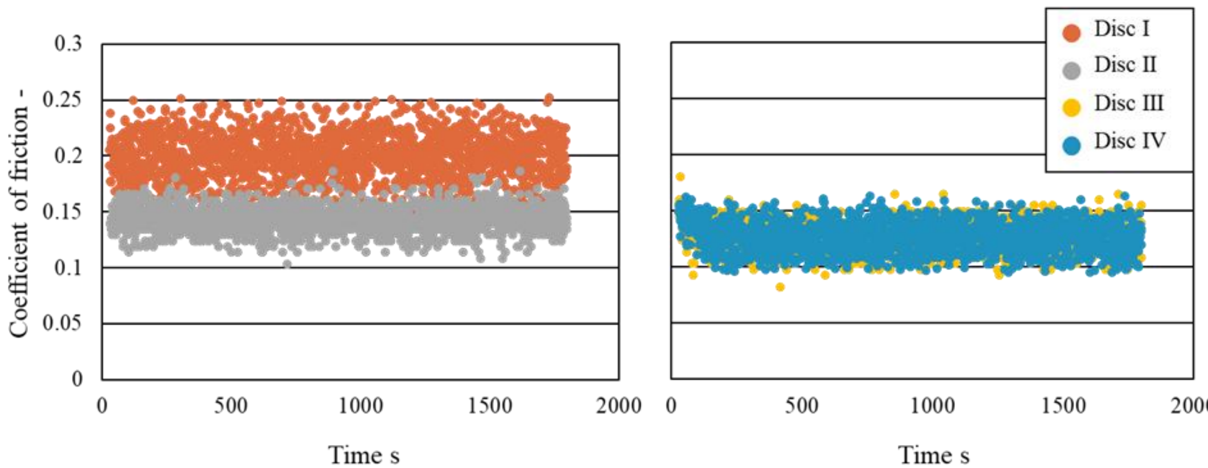

Figure 9: Relationship between elapsed time and coefficient of friction each disc.

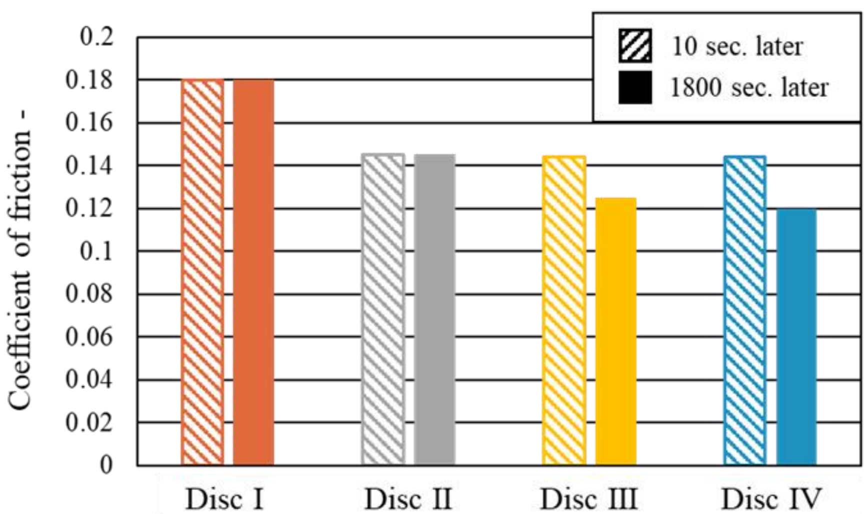

Figure 10: Coefficient of friction difference after 10 seconds and 1800 seconds.

CONCLUSIONS

In this study, to achieve the wear detecting by using simple solid lubricants, not using other special sensors, sulfides were used as a sensor of wear detecting. In particular, we found an advantage in detection speed compared to other detection mechanisms such as thermocouples and detecting coefficient of friction.

In the initial stage of about 10 or 60 seconds of friction, temperature changes of several degrees by thermocouples or temperature changes that cannot be detected by changes in the coefficient of friction can be supplemented by electromotive force detection using the thermoelectric conversion function of sulfide, a solid lubricant proposed in this study. This is considered to be the reason why this material has superior detection speed compared to other sensors.

After the friction has progressed sufficiently, it is clear that the electromotive force obtained depends on the amount of solid lubricant film formed. This is influenced by the difference in roughness of the mating material.

ACKNOWLEDGEMENT

A part of this research was financially supported by the Kansai University Fund for Domestic and Overseas Research Fund, 2023.

REFERENCES

Bhattacharya, S., Gunda, N.S.H., Stern, R., Jacobs, S., ChmielowskiR., Dennler, G., & Madsen, G.K.H. (2015). Achieving optimum carrier concentrations in p-doped SnS thermoelectrics. Phys.Chem.Chem.Phys.,17,9161-9166.

Ishikawa, S., Sato, T., Saitoh, K., Takuma, M., & Takahashi, Y., (2019). Fundamental study on functionality of synthetic sulfides: Evaluation of metal sulfides as solid lubricant. Jurnal Tribologi,20,26-38.

Liu, C., Yin, Y., Li, C., Xu, M., Li, R., & Chen,Q. (2021). Properties of lead-free copper matrix composites prepared through in situ Ni-coated FeS surface modification and mechanical alloying. Journal of alloys and compounds,881,160580, https://doi.org/10.1016/j.jallcom.2021.160580.

Liu, J., Goswami, A., Jiang., Khan, F., Kim, S., McGee, R., Li, Z., Hu, Z., Lee, J., & Thundat T. (2018). Direct-current triboelectricity generation by a sliding Schottky nanocontact on MoS2 multilayers. Nature nanotechnology,13,112-116.

Moghaddam, A.O., Shokuhfar,A., Guardia,P., Zhang,Y., & Cabot,A. (2019).Substantial role of doping in the thermoelectric and hardness properties of nanostructured bornite, Cu_5FeS_4. Journal of Alloys and Compounds. 773(30),1064-1074.

Mutton, P. J., & Watson, J. D. (1978). Some effects of microstructure on the abrasion resistance of metals. Wear, 48(2), 385-398.

Omoto, K., Ito H. (2012). Development of the Lubricating Oil Supply Unit with Self-power Generator. NTN Technical Review,80,48-51.

Österle, W., & Dmitriev, A.I. (2016). The role of solid lubricants for brake friction materials. Lubrication,4(5), doi:10.3390/lubricants4010005.

Sato,T., Ishikawa,S.,Saitoh,K.,Takuma, M., & Takahashi, Y. (2021). Evaluation of sulfides as solid lubricant: lubricity of compounded sulfides. Key engineering materials,901,164-169.

Sato, T., Yoshihara, M., Saitoh, K., Takuma, M., & Takahashi, Y. (2022). Material development for efficiently detecting the contact state of sulfide-based solid lubricants. Extended abstracts of 2022 JSME-IIP/ASME-ISPS joint international conference on micromechatronics for information and precision equipment (MIPE2022), B3-4-01.

Stachowiak, G. W. (2000). Particle angularity and its relationship to abrasive and erosive wear. Wear, 241(2), 214-219.

The Chemical Society of Japan(ed), Chemical Abstracts, 5th ed, (2004). I-731 (in Japanese).

Xue, F., Chen, L., Wang, L., Pang, Y., Chen, J., Zhang, C., & Wang, L. (2016). MoS_2 tribotronic transistor for smart tactile switch. Advanced functional materials.26,2104-2109. DOI: 10.1002/adfm.201504485.

Yin,Y., Li, R., Zhang, G., Zhang,K., Ding,S., & Chen Q. (2019). Tribological properties of FeS/Cu-Bi copper-based bearing materials fabricated by mechanical alloying. Industrial lubrication and tribology, 71(10),1152-1157., doi: 10.1108/ILT-03-2019-0106.

Zhu, J.,Gao,H.L.,Pi, D.N.,Xie, Z.Q. & Mei, L. (2019). Thermoelectric effect of wear of alloy bearing. Engineering Failure Analysis.103,376-383. https://doi.org/10.1016/j.engfailanal.2019.04.030.